Available online at www.sciencedirect.com
SCIENCE DIRECT
International Journal of Pharmaceutics 312 (2006) 1–14
INTERNATIONAL JOURNAL OF PHARMACEUTICS
www.elsevier.com/locate/ijpharm

Stability improvement of alpha-amylase entrapped in kappa-carrageenan beads: Physicochemical characterization and optimization using composite index

Mayur G. Sankalia, Rajshree C. Mashru *, Jolly M. Sankalia, Vijay B. Sutariya

Centre of Relevance and Excellence in Novel Drug Delivery Systems, Pharmacy Department, G.H. Patel Building, The M.S. University of Baroda, Vadodara 390002, India

Received 12 July 2005; received in revised form 1 November 2005; accepted 24 November 2005
Available online 24 February 2006

Abstract

Purpose: This work examines the influence of various process parameters on α-amylase entrapped in crosslinked κ-carrageenan beads for stability improvement. A three level full factorial design was employed to investigate the effect of three process variables namely κ-carrageenan concentration, potassium chloride concentration and hardening time on % entrapment, time required for 50% (T_{50}) and 90% (T_{90}) of enzyme release and particle size.

Methods: The beads were prepared by dropping the κ-carrageenan-containing α-amylase to magnetically stirred potassium chloride solution. The composite index was applied to optimize the process under study. 'In vitro' enzyme release profile of the beads was fitted to various release kinetics models to understand the release mechanism. Topographical characterization was carried out by SEM and entrapment was confirmed by FTIR and DSC. Stability testing according to the ICH guidelines for zone III and IV was carried out.

Results: With the use of ionotropic gelation method, a polymeric matrix prepared by 3.5% (w/v) κ-carrageenan, 0.7 M potassium chloride and hardening time of 30 min resulted in the production of beads characterized by disc shaped with collapsed center, absence of aggregates, % entrapment of 73.79, T_{90} of 74.4 min, and composite index of 83.01. Moreover, shelf-life of the enzyme loaded beads was found to increase up to 3.53 years compared to 0.99 year of the conventional formulation.

Conclusions: It can be inferred that the proposed method can be used to prepare α-amylase loaded κ-carrageenan beads for stability improvement. Also the proper selection of rate-controlling carrageenan concentration and its interactive potential for crosslinking is important and will determine the overall size and shape of beads, the duration and pattern of dissolution profiles and enzyme loading capacity.

Keywords: α-Amylase; κ-Carrageenan; Ionotropic gelation; Release kinetics; Composite index; Stability study

1. Introduction

α-Amylase, a major enzyme used for replacement of pancreatic enzymes, need not be reabsorbed in the intestine like other proteins, which are used for systemic therapy. Fungal α-amylases (EC 3.2.1.1; CAS 9000-90-2) are obtained from various strains of *Aspergillus* (mainly *A. niger*, *A. awamori*, and *A. usamii*) species. The α-amylases consist of three domains called A, B and C (Nielsen et al., 1999). The active site, situated in a cleft at the interface between domains A and B, is consist of three acids Asp231, Glu261 and Asp328, which are essential for catalytic activity (Uitdehaag et al., 1999). α-Amylases catalyze the hydrolysis of α-1,4 glycosidic linkages in starch and other related carbohydrates. α-Amylases are used in several industrial processes such as starch liquefaction, laundering, dye removal and feed preprocessing, but the largest volume is sold to the starch industry for the production of high-fructose syrups and ethanol (Guzman-Maldano and Paredes-Lopez, 1995).

Formulations containing α-amylase and other digestive enzymes need to be stored at cold (2–8 °C) or cool (8–25 °C) temperature conditions and still have the shelf-life of not more than 1 year. Entrapment of the α-amylase in ionotropically

* Corresponding author. Tel.: +91 265 2434187/2794051; fax: +91 265 2418927.
E-mail addresses: sankalia_mayur@hotmail.com (M.G. Sankalia), rajshree-mashru@yahoo.com (R.C. Mashru), jollymayur@hotmail.com (J.M. Sankalia).

0378-5173/$ – see front matter © 2006 Elsevier B.V. All rights reserved.
doi:10.1016/j.ijpharm.2005.11.048

crosslinked biodegradable hydrogels may improve the stability of the parent enzymes and make it less prone to interference of various formulation excipients. Immobilized enzymes are stable at higher temperature and might be stored at room temperature with extended shelf-life (Bickerstaff, 1997). Optimum pH for activity of α-amylase (*A. oryzae*) is 5.0 (Uhlig, 1998). Multiple unit dosage forms are particularly useful for delivery of enzymes, peptides/proteins and vaccines (Chen and Langer, 1997). Above advantages are of great commercial interest for the pharmaceutical industries hence it was the objective of the research to develop an extended shelf-life formulation of α-amylase by entrapment in ionotropically crosslinked biodegradable κ-carrageenan beads which results in better and efficient utilization of enzyme. This paper also deals with 'in vitro' dissolution studies and physicochemical characterization for evaluating the beads and its release behavior.

Carrageenan has been used increasingly in pharmaceutical formulation studies (Picker, 1999), for example, microcapsules for sustained delivery (Suzuki and Lim, 1994), crosslinked spheres for controlled release (Garcia and Ghaly, 1996; Sipahigil and Dortunc, 2001), or tablet for reducing inactivation of α-amylase (Schmidt et al., 2003). Carrageenans are naturally occurring high molecular weight polysaccharides extracted from red seaweed. They are made up of alternating copolymers of 1,3-linked β-D-galactose and 1,4-linked 3,6-anhydro-α-D-galactose. The units are joined by alternating α-1,4 and β-1,4 glycosidic linkages. Depending on the algae from which they are extracted and the preparative technique, three main types of carrageenans (Scheme 1) are available; kappa (κ), lambda (λ), and iota (ι). Because of the ionic nature of the polymer, gelation is strongly influenced by the presence of electrolytes. κ-Carrageenan forms a gel with potassium ions, but also shows gelation under salt-free conditions. However, gels prepared in the presence of metallic ions were substantially stronger than those obtained under salt-free conditions (Hossain et al., 2001). The gelling and melting temperatures of κ-carrageenan are dependent almost solely on the concentration of potassium ions.

When a polyelectrolyte (like carrageenan) is combined with a uni/multivalent ion of the opposite charge, it may form a physical hydrogel known as an 'ionotropic' hydrogel. Ionotropic hydrogel, which may degrade and eventually disintegrate and dissolve, are held together by molecular entanglements, and/or secondary forces including ionic, H-bonding or hydrophobic forces (Prestwich et al., 1998). All of these interactions are reversible, and can be disrupted by changes in physical conditions such as ionic strength, pH, temperature, application of stress, or addition of specific solutes that compete with the polymeric ligand for the affinity site on the protein.

From these characteristics, κ-carrageenan is used as an entrapment matrix for cells and enzymes as well as for pharmaceuticals and food adjuvants. In the past, conventional crosslinked potassium-κ-carrageenan beads have been investigated for the development of a multiple unit drug delivery system. However, not even a single reference could be cited in literature till date for entrapment of α-amylase in κ-carrageenan beads for improvisation of shelf-life, hence it was the objective of the study.

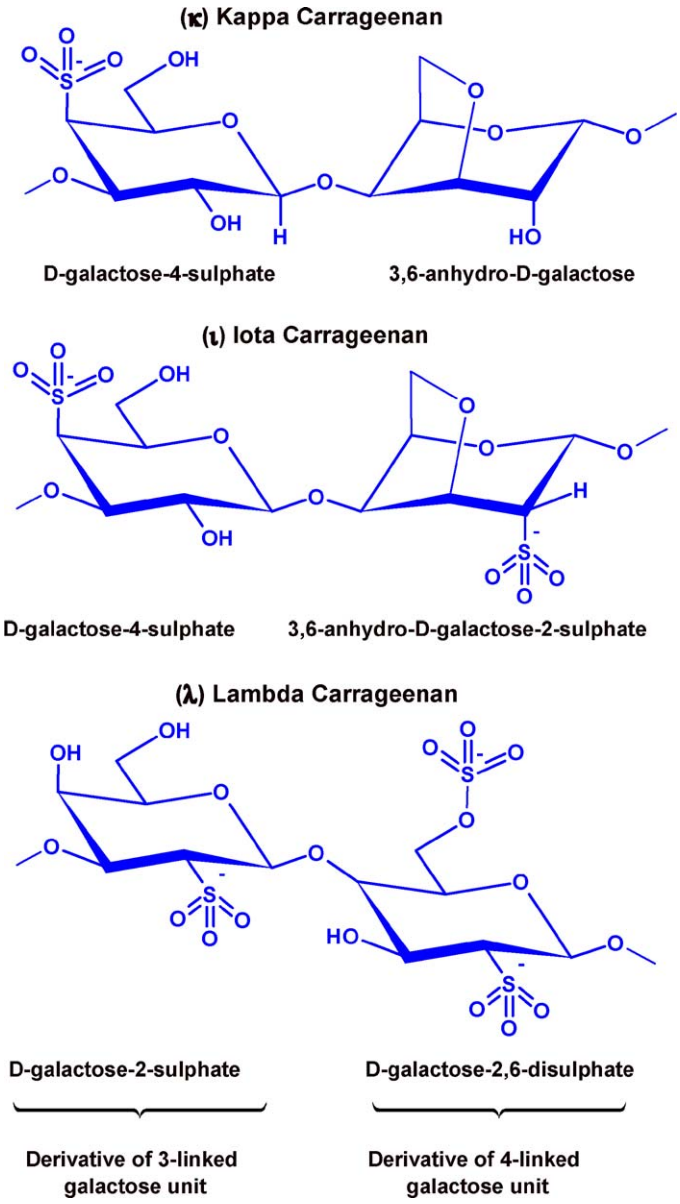

Scheme 1. Different types of carrageenan.

2. Materials and methods

2.1. Materials

Potassium dihydrogen phosphate, sodium hydroxide, hydrochloric acid (Qualigens Fine Chemicals, Mumbai, India) and soluble starch (Himedia Laboratories Pvt. Ltd., Mumbai, India) were used as received. Fungal α-amylase, κ-carrageenan (obtained from Irish moss, *Chondrus crispus*), potassium chloride, iodine, and potassium iodide were purchased from S.D. Fine-Chem Ltd., Mumbai, India. All the other chemicals and solvents were of analytical grade and were used without

further purification. Deionized double-distilled water was used throughout the study.

2.2. Characterization of carrageenan

The carrageenan procured was derived from Irish moss (*C. crispus*), which is known to contain kappa (gelling fraction) and lambda (non-gelling fraction) carrageenan as major constituents. Carrageenan sample was tested according to the identification test B (gel constancy test) and D (FTIR study) of USP-27 NF-22, and was found to be kappa-carrageenan with non-gelling fraction (lambda-carrageenan) of less than 5%. Moreover, the kappa-carrageenan was confirmed by observing the syneresis phenomenon, which is not observed with iota-carrageenan gels.

2.3. Preparation of beads

Concentrated κ-carrageenan solution in distilled water was prepared by heating the powder dispersion at 70 °C to get homogenous solution and cooled to 40 °C. Required quantity of enzyme (200 mg α-amylase in 50 ml of final κ-carrageenan solution) was dissolved in small quantity of water and mixed with concentrated κ-carrageenan solution. Final concentration of κ-carrageenan was adjusted in the range of 2.5–3.5% (w/v) and was used after being degassed under vacuum. The beads were prepared by dropping the κ-carrageenan solution (10 ml) containing α-amylase from the dropping device such as syringe with 18-G × 1/2 in. flat-tip hypodermic needle to a magnetically stirred potassium chloride solution (40 ml) at a rate of 5 ml/min and were allowed to harden for specific time. Different levels (Table 1) of κ-carrageenan, potassium chloride and hardening time were selected. The beads were collected by decanting potassium chloride solution, washed with deionized water and dried to a constant weight in vacuum desiccator (Tarsons Products Pvt. Ltd., Kolkata, India) at room temperature for 48 h.

2.4. Factorial design

Before the application of the design, number of preliminary trials were conducted by changing one variable at a time and keeping other variables fixed to determine the conditions at which the process resulted to beads. In the present study three-level full factorial design (FFD) was employed to generate response surfaces. To determine the experimental error, the experiment at the centre point was repeated five times at different days. The mean % entrapment, T_{50}, T_{90}, and particle size at the center-replicated points were $73.96 \pm 0.46\%$, 33.64 ± 0.65 min, 44.12 ± 1.21 min, and 1.92 ± 0.008 mm, respectively and showed good reproducibility of the process. The quadratic coefficients were estimated using the least-squares multiple regression to the observed response. The analysis of variance (ANOVA) was performed in order to determine significance of the fitted equation. All analytical treatments were supported by NCSS software. The process variables with their coded experimental values and the results of the responses are reported in Table 2.

Table 1
Process variables and their levels for 3^3 full factorial design

Factors	Coded levels	Actual levels
A: κ-carrageenan concentration (%, w/v)	−1	2.5% (w/v)
	0	3.0% (w/v)
	1	3.5% (w/v)
B: potassium chloride concentration (M)	−1	0.3 M
	0	0.5 M
	1	0.7 M
C: hardening time (min)	−1	10 min
	0	20 min
	1	30 min

2.5. Composite index

On completion of the individual experiments, a weighted composite index was used to designate a single score utilizing two responses, i.e., % entrapment, and T_{90}. Many researchers have utilized the technique of multiple responses for optimization studies. Derringer and Suich illustrated how several response variables can be transformed into one response (Derringer and Suich, 1980). The applications of one-sided transformations are also demonstrated by different researchers (Bodeam and Leucata, 1997; Gohel et al., 2003). The application of generalized distance function to incorporate several objectives into a single function has been reported (Shigeo et al., 1994). As the relative contribution of each individual constraint to the "true" composite score was unknown, a decision was made to assign an arbitrary value of one-half to each of the two response variables (Taylor et al., 2000). The empirical composite index was devised to yield a score 100 for an optimum result for each of the two responses and each formulation result was transformed to a value between 0 and 50. For % entrapment, highest value (84.7) was assigned a score equal to 50, and lowest value (52.59) was assigned zero score. For T_{90}, lowest value (25.5) was assigned to zero score and the highest value (74.4) was assigned to 50. The batch having the highest composite index would be considered as a batch fulfilling the desired criteria. The raw data transformations were as follows:

$$\text{transformed value of \% entrapment or } T_{90} = \frac{Y_i - Y_{\min}}{Y_{\max} - Y_{\min}} \times 50 \quad (1)$$

where Y_i is the experimental value of individual response variable, $Y_{\max}$ and $Y_{\min}$ are maximum and minimum values of individual response variable, respectively.

$$\text{composite index} = \text{transformed value of \% entrapment} + \text{transformed value of } T_{50} \quad (2)$$

2.6. Curve fitting

The 'in vitro' release pattern was evaluated to check the goodness of fit to the zero-order release kinetics Eq. (3), first-order

Table 2
Factorial 3^3: matrix of the experiments and results for the measured responses and the composite index

ES[a]	Factors/levels			Responses				Transformed		Composite index (CI)
	Carrageenan (%, w/v)	KCl (M)	Hardening time (min)	% Immobilization	T_{50}	T_{90}	Particle size ± S.D.[b] (mm)	% Immobilization	T_{90}	
9	−1	−1	−1	65.34	17.15	25.50	1.83 ± 0.19	19.85	50.00	19.85
13	−1	−1	0	62.40	19.20	29.70	1.80 ± 0.17	15.28	45.71	19.57
2	−1	−1	1	60.29	22.10	33.65	1.76 ± 0.18	11.99	41.67	20.32
24	−1	0	−1	62.11	22.30	32.50	1.68 ± 0.20	14.82	42.84	21.98
17	−1	0	0	59.25	25.45	38.60	1.65 ± 0.19	10.37	36.61	23.77
6	−1	0	1	57.24	29.10	44.10	1.61 ± 0.20	7.24	30.98	26.26
1	−1	1	−1	57.27	28.86	42.35	1.63 ± 0.19	7.29	32.77	24.52
27	−1	1	0	54.49	32.65	46.10	1.60 ± 0.20	2.96	28.94	24.02
10	−1	1	1	52.59	36.40	49.70	1.56 ± 0.17	0.00	25.26	24.74
23	0	−1	−1	78.79	24.50	35.30	2.09 ± 0.20	40.80	39.98	50.82
8	0	−1	0	75.97	28.75	41.10	2.06 ± 0.16	36.41	34.05	52.36
15	0	−1	1	73.96	33.05	46.05	2.02 ± 0.17	33.28	28.99	54.29
12	0	0	−1	76.65	30.75	41.50	1.95 ± 0.20	37.46	33.64	53.82
26	0	0	0	73.92	33.70	44.15	1.92 ± 0.19	33.21	30.93	52.28
19	0	0	1	72.02	37.75	50.90	1.88 ± 0.20	30.26	24.03	56.23
3	0	1	−1	70.68	37.86	50.83	1.90 ± 0.22	28.17	24.10	54.07
18	0	1	0	68.00	42.05	55.20	1.87 ± 0.19	24.00	19.63	54.36
21	0	1	1	66.18	44.60	62.95	1.83 ± 0.18	21.16	11.71	59.45
4	1	−1	−1	84.70	31.50	45.40	2.43 ± 0.19	50.00	29.65	70.35
25	1	−1	0	82.02	35.90	49.30	2.41 ± 0.19	45.83	25.66	70.16
11	1	−1	1	80.13	40.95	56.20	2.38 ± 0.18	42.88	18.61	74.27
22	1	0	−1	82.30	38.47	51.90	2.29 ± 0.17	46.26	23.01	73.26
14	1	0	0	79.79	42.10	56.05	2.27 ± 0.19	42.35	18.76	73.59
7	1	0	1	78.03	45.50	62.00	2.24 ± 0.19	39.61	12.68	76.93
5	1	1	−1	77.80	45.60	60.50	2.26 ± 0.18	39.26	14.21	75.04
16	1	1	0	75.42	48.30	67.80	2.24 ± 0.18	35.55	6.75	78.80
20	1	1	1	73.79	51.40	74.40	2.21 ± 0.18	33.01	0.00	83.01

[a] ES, experimental sequence.
[b] S.D., standard deviation ($n = 50$).

release kinetics (Gibaldi and Feldman, 1967; Wagner, 1969) Eq. (4), Higuchi's square root of time equation (Higuchi, 1963) Eq. (5), Korsmeyer–Peppas' power law equation (Korsmeyer et al., 1983; Peppas, 1985) Eq. (6), and Hixson–Crowell's cube root of time equation (Hixson and Crowell, 1931) Eq. (7). The goodness of fit was evaluated by r (correlation coefficient) values. For better understanding residual analysis (Pather et al., 1998) of above models was performed on the optimized formulation

$$Q_t = Q_0 + K_0 t \tag{3}$$

where Q_t is the amount of drug dissolved in time t, Q_0 is the initial amount of drug in the solution (most times, $Q_0 = 0$), K_0 is the zero order release constant and t is release time

$$Q_t = Q_0 \, e^{-K_1 t} \tag{4}$$

where Q_t is the amount of drug dissolved in time t, Q_0 is the initial amount of drug in the solution, K_1 is the first order release constant and t is release time

$$Q_t = K_H \sqrt{t} \tag{5}$$

where Q_t is the amount of drug dissolved in time t, K_H is the Higuchi dissolution constant and t is release time

$$\frac{Q_t}{Q_\infty} = K_k t^n \tag{6}$$

where Q_t is the amount of drug dissolved in time t, Q_∞ is the amount of drug dissolved in ∞ time (the drug loaded in the formulation), Q_t/Q_∞ is the fractional release of the drug in time t, K_k is a constant incorporating structural and geometric characteristic of dosage form, n is the release (diffusional) exponent that depends on the release mechanism and the shape of the matrix tested (Ritger and Peppas, 1987) and t is release time. Interpretation of diffusional exponent is given in Table 3

$$Q_0^{1/3} - Q_t^{1/3} = K_s t \tag{7}$$

Table 3
Interpretation of Korsmeyer–Peppas power law release exponent

Release exponent (n)	Drug transport mechanism	Rate as a function of time
0.5	Fickian diffusion	$t^{-0.5}$
$0.5 < n < 1.0$	Anomalous transport	t^{n-1}
1.0	Case-II transport	Zero order release
Higher than 1.0	Super case-II transport	t^{n-1}

where Q_0 is the initial amount of drug in the pharmaceutical dosage form, Q_t is the remaining amount of drug in pharmaceutical dosage form at time t, K_s is a constant incorporating the surface–volume relation and t is release time.

In order to understand the release mechanism, the release data of the optimized batch was fitted to empirical equations proposed by Kopcha (Kopcha et al., 1991) Eq. (8)

$$M = At^{1/2} + Bt \tag{8}$$

In the above equations, M ($\leq$70%) is the percentage of drug released at time t, while A and B are, respectively, diffusion and erosion terms. According to this equation, if diffusion and erosion ratio, $A/B = 1$, then the release mechanism includes both diffusion and erosion equally. If $A/B > 1$, then diffusion prevails, while for $A/B < 1$, erosion predominates.

2.7. Characterization of beads

2.7.1. Estimation of α-amylase (dextrinogenic assay)

The iodine test of Smith and Roe (Smith and Roe, 1957; Hsiu et al., 1964) was modified as follows: 2 ml of a 0.2% starch solution was added to 1.0 ml of enzyme diluted in 0.05 M phosphate buffer pH 6.8. The mixture was incubated for 3 min at 25° and then reaction was stopped with 1 ml of 1 N HCl. Finally, 20 ml of water and 0.5 ml of 0.01 N iodine solution prepared according to Rice (1959) were added and the absorbance A was recorded on a spectrophotometer (Shimadzu UV-1601, Japan) at 660 nm. The instrument was adjusted to zero reading with iodine blank containing neither enzyme nor substrate. The dextrinogenic activity is expressed in arbitrary units as follows:

$$D = \frac{A_B - A}{A_B} E \tag{9}$$

where A_B is the absorbance of the starch–iodine complex in the absence of enzyme and E is the enzyme dilution. Best results were obtained when the enzyme solution was diluted in such a manner as to make the ratio $(A_B - A)/A_B$, approach 0.20–0.25.

2.7.2. Determination of entrapment efficiency

Entrapment efficiency was determined by dissolving the enzyme loaded beads in a magnetically stirred simulated gastric fluid (SGF) without enzyme (USP XXVI) for about 90 min. An aliquot of 2 ml was taken and neutralized to pH 6.8 using 0.01 N sodium hydroxide. The resulting solution was centrifuged at 2500 rpm for 10 min (Remi Instruments Ltd., Mumbai, India) and supernatant was assayed ($n = 3$) for enzyme content by dextrinogenic assay as above. Entrapment efficiency was calculated as

$$\text{entrapment efficiency} = \frac{\text{enzyme loaded}}{\text{theoretical enzyme loading}} \times 100 \tag{10}$$

2.7.3. Determination of T_{50} and T_{90}

Time required for 50 (T_{50}) and 90 (T_{90}) percent of enzyme release were used to evaluate the onset and duration of action, respectively. For optimization purpose, dissolution study of all batches was carried out in 500 ml of SGF without enzyme using the USP XXVI dissolution apparatus 2 (TDT-60T, Electrolab, Mumbai, India) at 37 ± 0.5 °C with paddle speed of 75 rpm. Accurately weighed samples ($n = 3$) equivalent to about 40 mg of α-amylase were subjected to dissolution and aliquots of 2 ml were collected, neutralized to pH 6.8 using 0.01 N sodium hydroxide, and assayed at 0, 5, 10, 15, 20, 30, 45, 60, 90 and 120 min. T_{50} and T_{90} were found by extrapolating the % enzyme released versus time plot.

2.7.4. Particle size measurements

The particle sizes of 50 gel beads were measured with a gauge type micrometer (0.01 mm least count, Durga Scientific Pvt. Ltd., Vadodara, India) for each formulation and the mean particle size was determined.

2.7.5. Fourier transform infra-red spectroscopy (FTIR)

IR transmission spectra were obtained using a FTIR spectrophotometer (FTIR-8300, Shimadzu, Japan). A total of 2% (w/w) of sample, with respect to the potassium bromide (KBr; S.D. Fine-Chem Ltd., Mumbai, India) disc, was mixed with dry KBr. The mixture was ground into a fine powder using an agate mortar before compressing into KBr disc under a hydraulic press at 10,000 psi. Each KBr disc was scanned at 4 mm/s at a resolution of 2 cm over a wavenumber region of 400–4000 cm^{-1}. The characteristic peaks were recorded.

2.7.6. Differential scanning calorimetry (DSC)

Differential scanning calorimetric analysis was used to characterize the thermal behavior of the isolated substances, empty and enzyme loaded beads. DSC thermograms were obtained using an automatic thermal analyzer system (DSC-60, Shimadzu, Japan). Temperature calibration was performed using indium as a standard. Samples were crimped in a standard aluminum pan and heated from 40 to 400 °C at a heating rate of 10 °C/min under constant purging of dry nitrogen at 30 ml/min. An empty pan, sealed in the same way as the sample, was used as a reference.

2.7.7. Scanning electron microscopy (SEM)

The purpose of SEM study was to obtain a topographical characterization of beads. The beads were mounted on brass stubs using carbon paste. SEM photographs were taken with scanning electron microscope (JSM-5610LV, Jeol Ltd., Japan) at the required magnification at room temperature. The working distance of 39 mm was maintained and acceleration voltage used was 5 kV, with the secondary electron image (SEI) as a detector.

2.8. Preparation of capsule formulation, packaging, and stability study

Accurately weighed carrageenan beads equivalent to 40 mg of α-amylase were filled into a hard gelatin capsule manually. The joint of the capsule body and cap was carefully sealed by pressing them to fit in the lock mechanism. The capsules

were packed in high density polyethylene (HDPE) bottles with polypropylene (PP) caps (foamed polyethylene and pressure sensitive liner). The capsules were subjected to stability testing according to the International Conference on Harmonization guidelines for zone III and IV. The packed containers of prepared capsules along with marketed formulation and bulk α-amylase were kept for accelerated ($40 \pm 2\,^{\circ}C/75 \pm 5\%$ relative humidity) and long term ($30 \pm 2\,^{\circ}C/65 \pm 5\%$ relative humidity) stability in desiccators with saturated salt solutions for up to 12 months. For accelerated and long term stability, desiccators containing saturated sodium chloride and potassium iodide solutions were kept into ovens at 40 and 30 °C to maintain a constant relative humidity of 74.68 ± 0.13 and 67.98 ± 0.23, respectively. A visual inspection (for discoloration of capsule content), dissolution testing and α-amylase content estimation was carried out every 15 days for the entire period of stability study.

3. Results and discussion

3.1. Effect of the factors on responses

3.1.1. % Entrapment

ANOVA results and regression coefficients of response variables are shown in Table 4. All three process variables were statistically significant ($P < 0.05$). From the contour plots of response surface for % entrapment (Fig. 1A–C) and Table 2, it can be concluded that concentration of κ-carrageenan was the most influencing factor (45.53%) and affecting positively (positive coefficient; Table 4; i.e. response increases with increase in factor level). However, potassium chloride concentration and hardening time were affecting negatively (negative coefficient; Table 4; i.e. response decreases with increase in factor level) in significant amount. More than 84% entrapment (experiment 4) was obtained at the high level of the κ-carrageenan concentration especially when it was followed by the low levels of the other two factors.

On addition of κ-carrageenan solution to a potassium chloride solution, instantaneous interfacial crosslinking takes place followed by a more gradual gelation of the interior and causes loss of enzyme from the beads, which was found to be proportional to the degree of crosslinking. Increase in viscosity with increase in κ-carrageenan concentration may retard penetration of potassium to the interior of the bead, resulted in decreased crosslinking (also decreased surface roughness and porosity; Fig. 2D and E) and hence increased entrapment efficiency. Degree of crosslinking increased with increase in potassium concentration and contact time, and so entrapment efficiency decreased. The entrapment efficiency of the α-amylase containing beads prepared with calcium alginate (sodium alginate and calcium chloride) and chitosan-alginate was 91% and 90%, respectively, using κ-carrageenan the α-amylase entrapment efficiency in our study did not exceed 85%, although the same method was used. So with chitosan or alginate more efficient entrapment was achieved (Bodmeier and Wang, 1993).

3.1.2. T_{50} and T_{90}

As shown in Fig. 1 and Table 4, all three factors had significant positive effect on both response values. The concentration of κ-carrageenan concentration (factor *A*) had the most significant effect. For maximum activity of enzyme in the intestine, longer T_{50} and T_{90} were the desired criteria for the optimum formulation. Thus, extreme level of all three variables resulted the beads with T_{50} and T_{90} as high as 51.4 and 74.4 min, respectively (experiment 20, Table 2). T_{50} and T_{90} were found to be proportional to particle size and degree of crosslinking. As the concentration and hence the viscosity of κ-carrageenan incereases, larger beads (discussed under 'particle size') were obtained which took long time for complete dissolution and resulted in higher T_{50} and T_{90}. The increase of the in vitro release rates of α-amylase from carrageenan beads prepared with low concentrations of potassium chloride solutions may be due to the less crosslinked structure of the beads which may result in a more porous matrix (Fig. 2A–C) and higher drug release (Garcia

Table 4
ANOVA results (*P* values): effect of the variables on % entrapment, T_{50}, T_{90}, particle size and composite index

Factors	% Entrapment		T_{50}		T_{90}		Particle size		Composite index	
	Coefficient	*P*	Coefficient	*P*	Coefficient	*P*	Coefficient	*P*	Coefficient	*P*
Intercept	73.73	<0.0001*	33.97	<0.0001*	45.10	<0.0001*	1.92	<0.0001*	52.96	<0.0001*
A	10.17	<0.0001*	8.14	<0.0001*	10.08	<0.0001*	0.31	<0.0001*	26.13	<0.0001*
B	−3.74	<0.0001*	6.37	<0.0001*	8.20	<0.0001*	−0.09	<0.0001*	2.56	<0.0001*
C	−2.30	<0.0001*	3.55	<0.0001*	5.23	<0.0001*	−0.03	<0.0001*	1.77	<0.0001*
A^2	−3.85	<0.0001*	−0.58	0.0068*	0.98	0.0929	0.04	<0.0001*	−4.99	<0.0001*
B^2	−1.37	<0.0001*	0.74	0.0009*	2.03	0.0016*	0.05	<0.0001*	−0.06	0.8971
C^2	0.30	0.0609	0.24	0.2173	0.98	0.0939	−0.005	0.0126*	1.47	0.0060*
AB	0.32	0.0120*	−0.21	0.1672	0.21	0.6308	0.008	<0.0001*	0.71	0.0664
AC	0.15	0.2228	0.25	0.1032	0.64	0.1484	0.005	0.0025*	0.88	0.0256*
BC	0.10	0.3757	−0.24	0.1169	0.30	0.4820	0.000	1.0000	0.48	0.2083
ABC	0.02	0.8688	−0.78	0.0003*	0.49	0.3622	0.000	1.0000	0.54	0.2466
$r^2_{adj.}$	0.9979	–	0.9965	–	0.9820	–	0.9996	–	0.9962	–

Regression coefficients are in coded values.
* Statistically significant ($P < 0.05$).

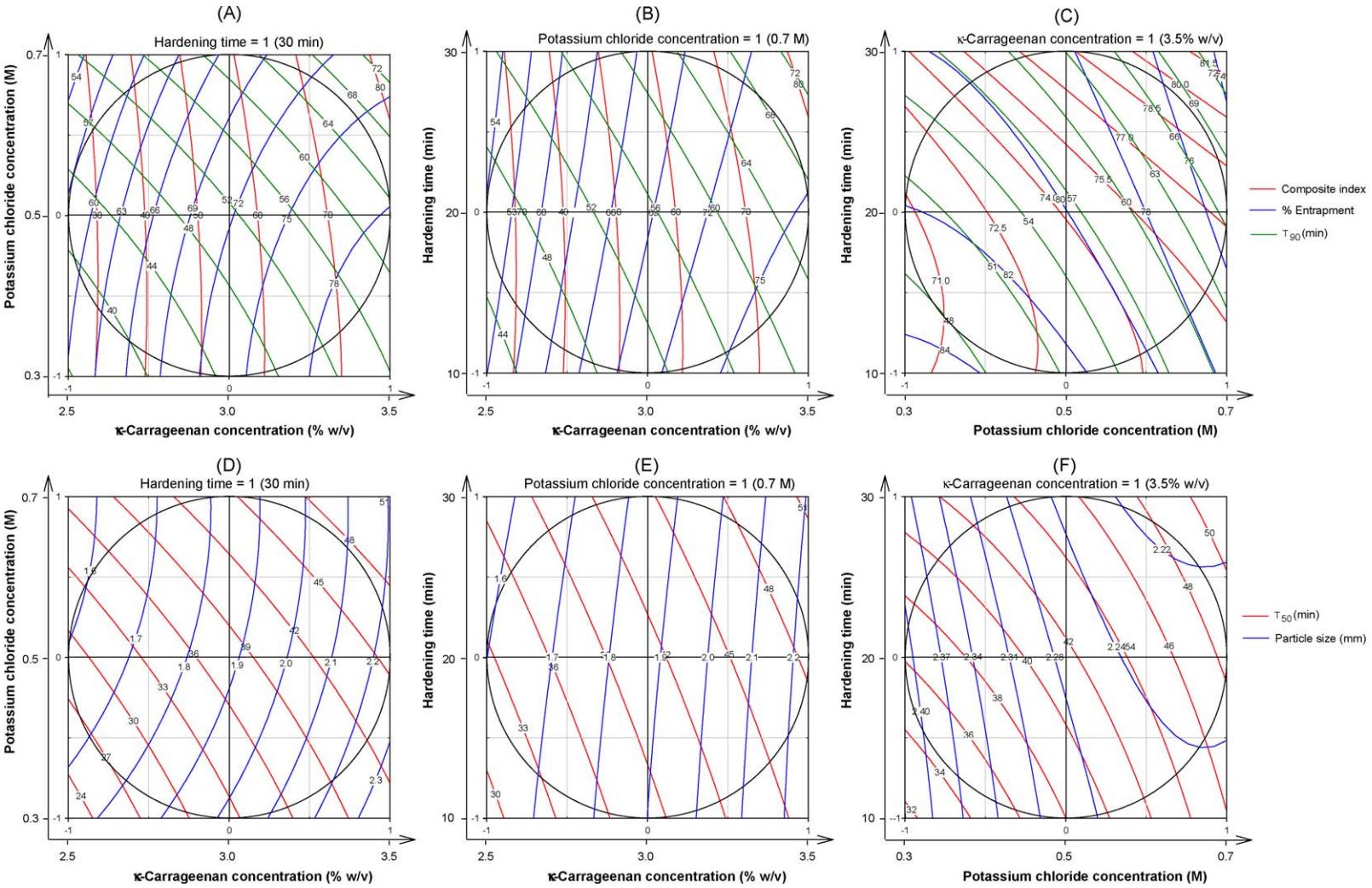

Fig. 1. Contour plots of composite index, % entrapment, T_{90}, T_{50}, and particle size as a function of κ-carrageenan concentration, potassium chloride concentration, and hardening time.

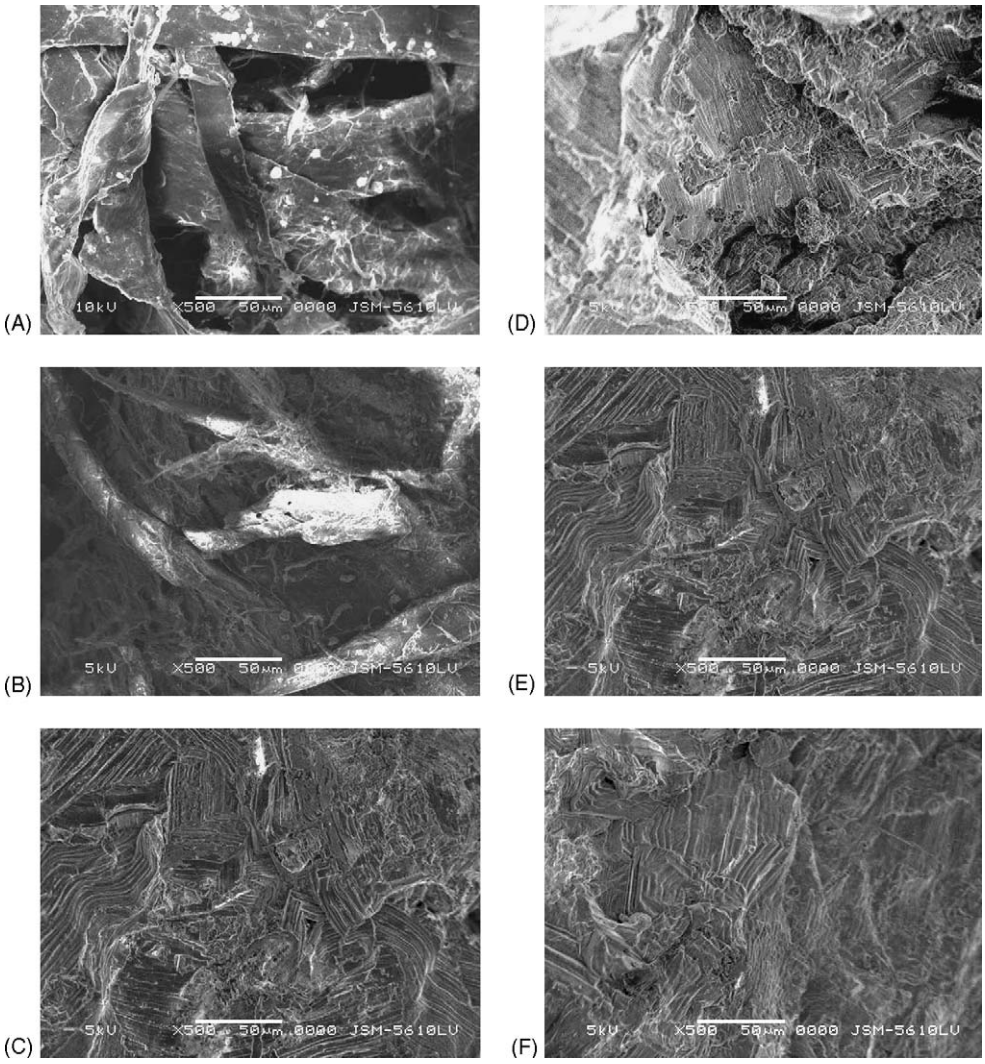

Fig. 2. SEM micrographs and surface morphology of carrageenan beads: (A–C) Effect of potassium chloride concentration (κ-carrageenan concentration 3.0%, w/v) (A) 0.3 M, (B) 0.5 M, and (C) 0.7 M potassium chloride concentration. (D–F) Effect of κ-carrageenan concentration (potassium chloride concentration 0.7 M) (D) 2.5%, w/v, (E) 3.0%, w/v, and (F) 3.5%, w/v κ-carrageenan concentration.

and Ghaly, 1996; Sipahigil and Dortunc, 2001). Higher hardening time caused penetration of potassium to the interior of the bead, resulted in increased crosslinking, and hence higher T_{50} and T_{90}.

3.1.3. Particle size

As depicted in Table 4, the κ-carrageenan concentration (factor *A*; most influential; 56.77%) had positive coefficient, while potassium chloride concentration and hardening time had negative coefficient. In contrast to the finding of Sipahigil (Sipahigil and Dortunc, 2001) and Bhardwaj (Bhardwaj et al., 1995), all three process variables were statistically significant ($P < 0.05$). Freely water soluble drug always entrapped in higher ratio and results in bigger particles (Sipahigil and Dortunc, 2001). The bead size is influenced by the opening through which the κ-carrageenan is allowed to pass (which was kept constant) and the viscosity of the carrageenan solution. Increased viscosity at higher concentration of κ-carrageenan resulted in larger particles. High potassium chloride concentration and hardening time resulted in smaller particle size due to high degree of crosslinking. Though the negative effect of potassium chloride concentration and hardening time was of less magnitude, they contribute to the morphology of the beads (Fig. 2A–C).

3.2. Interactions between the factors

An interaction is the failure of a factor to produce the same effect on the response at the different levels of the other factor. The ANOVA results (Table 4) showed that interaction AB had significant influence on % entrapment, ABC had significant influence on T_{50}, while AB and AC had significant influence on particle size. The analysis of the results by multiple regression (Table 4) leads to equations that adequately describe the influence of the selected factors on % entrapment, T_{50}, T_{90}, particle size, and composite index.

3.3. Optimization of the process using the composite index

Generally the aim of the optimization is to find the optimum levels of the variables, which affect a process, where a product of desired characteristics could be produced easily and reproducibly. Using the composite index, both selected responses (% entrapment and T_{90}) were combined in one response. As it has been already discussed, the composite index was calculated from the individually calculated transformed value of each of the responses using the Eqs. (1) and (2). The equation found out using multiple regression was as follow (coded factors):

$$\mathrm{CI} = 62.87 + 5.53A - 14.22B - 8.93C - 7.00A^2 - 4.22B^2 - 0.53C^2 + 0.28AB - 0.43AC - 0.15BC - 0.46ABC \quad (r^2_{\mathrm{adj.}} = 0.9822,\ P < 0.0001) \qquad (11)$$

In Fig. 1A–C the contour plots that describe the influence of the independent factors on the composite index is presented. The study of these plots and Table 2 showed that the highest values of the CI (83.01) could be obtained at high level of all three independent factors (experiment 20) and was considered as a batch fulfilling all the constraints favorable for the bead preparation.

3.4. Evaluation of model using cross-validation

In order to assess the reliability of the model, five experiments were conducted by varying the process variables at values other than that of the model. For each of these test experiments the responses were estimated by using the multiple regression equations and experimental procedure for comparison between both responses (Table 5). Bias was calculated by the following equation:

$$\mathrm{bias} = \left[\frac{\text{predicted value} - \text{experimental value}}{\text{predicted value}}\right] \times 100 \qquad (12)$$

It can be seen that in all cases there was a reasonable agreement between the predicted and the experimental value, since low value of the bias were found. For this reason it can be concluded that the equations describe adequately the influence of the selected process variables on the responses under study.

3.5. Curve fitting and release mechanism

'In vitro' dissolution profile of the optimized batch is shown in Fig. 3A. Release of α-amylase from κ-carrageenan beads in simulated gastric fluid is conceivably attributed to the presence of strongly acidic sulphate groups in the carrageenan molecule, that allow a certain degree of ionization to be maintained also at low pH (Bonferoni et al., 1994). Values of release expo-

Table 5
Comparison of responses between predicted and experimental values for the cross-validation set

Responses	Test	Factors/levels			Experimental values	Predicted values	Bias %
		A	*B*	*C*			
% Entrapment	1	−1	−0.6	−0.6	63.26	62.50	1.2
	2	−0.6	0	0.4	65.34	63.70	2.5
	3	−0.4	0.6	0	66.23	68.08	−2.8
	4	0	−0.4	0.6	73.71	71.79	2.6
	5	0.4	0.4	−0.4	76.44	78.28	−2.4
T_{50}	1	−1	−0.6	−0.6	19.88	20.44	−2.8
	2	−0.6	0	0.4	30.28	31.10	−2.7
	3	−0.4	0.6	0	34.76	33.68	3.1
	4	0	−0.4	0.6	33.82	34.66	−2.5
	5	0.4	0.4	−0.4	38.44	37.96	1.2
T_{90}	1	−1	−0.6	−0.6	29.48	29.22	0.9
	2	−0.6	0	0.4	41.51	42.39	−2.1
	3	−0.4	0.6	0	46.83	46.09	1.6
	4	0	−0.4	0.6	45.57	46.66	−2.4
	5	0.4	0.4	−0.4	50.81	51.37	−1.1
Particle size	1	−1	−0.6	−0.6	1.75	1.71	2.1
	2	−0.6	0	0.4	1.73	1.76	−1.8
	3	−0.4	0.6	0	1.76	1.74	1.3
	4	0	−0.4	0.6	1.94	1.98	−2.2
	5	0.4	0.4	−0.4	2.03	2.06	−1.6
Composite index	1	−1	−0.6	−0.6	20.69	19.24	7.0
	2	−0.6	0	0.4	36.22	34.58	4.5
	3	−0.4	0.6	0	43.05	45.19	−4.9
	4	0	−0.4	0.6	53.41	51.54	3.5
	5	0.4	0.4	−0.4	63.02	66.45	−5.4

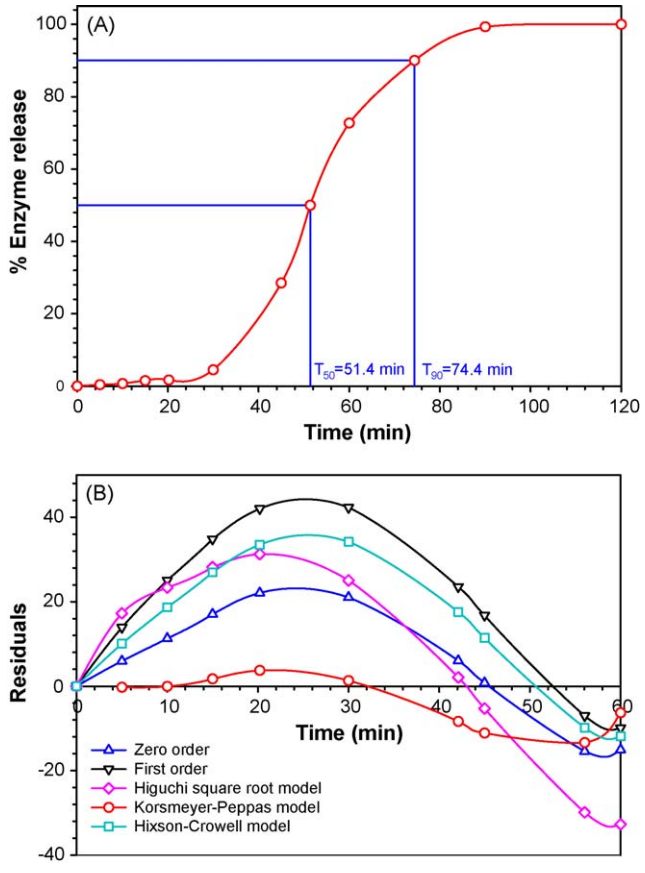

Fig. 3. (A) 'In vitro' release profile of optimized formulation (experiment 20) in SGF without enzyme. (B) Residual plot of different release models for the same formulation.

nent (n) and kinetic constant (K) were derived using Eqs. (3) to (7) and are presented in Table 6. The enzyme release data show a good fit to the Korsmeyer–Peppas' power law release kinetics Eq. (6), which can be confirmed by comparing the values of correlation coefficient (r) with that of the other models. The values of Korsmeyer–Peppas' release exponent (n) determined for the various formulations studied ranged from 1.29 to 2.42 suggesting the probable release by super case-II transport. The K_k values ranged from 0.0033 to 1.22 where low K_k value may suggest near to zero release from the beads initially. If one considers the correlation coefficient (r) values of zero-order and Korsemeyer–Peppas release models, both models describe the dissolution data reasonably well. Where there are competing models (with similar r values), residuals analysis can be used to distinguish between the models (Pather et al., 1998). Fig. 3B is the residual plot for optimized formulation. The residuals are high for the zero-order, first-order, Higuchi, and Hixson–Crowell models (and least for the Korsemeyer–Peppas model), which also shows systematic deviation: the models overpredict initially and underpredict at the later stages of the dissolution process. This indicates that Korsemeyer–Peppes' power low is the best fit model in describing the dissolution behavior of α-amylase from κ-carrageenan beads.

Finally, in order to know whether the enzyme release was due to erosion or diffusion, the release data of the optimized formulation was fitted to Kopcha model Eq. (8) and parameters like A and B at different time intervals were determined (Fig. 4). Throughout the release profile, A was <0 and B was >0, and expressed the predominance of erosion relative to diffusion. This probably may be due to the lower gel strength of carrageenan gels. During dissolution study carrageenan gel swell but is unable to maintain the gel matrix due to low gel strength and start to erode. However, the rate of hydration initially was found to be the rate limiting step of erosion rate and explain the biphasic nature of release profile (plateau initially followed by steep rise in erosion rate). The erosion term B increases with time because erosion of the hydrated layer is easier.

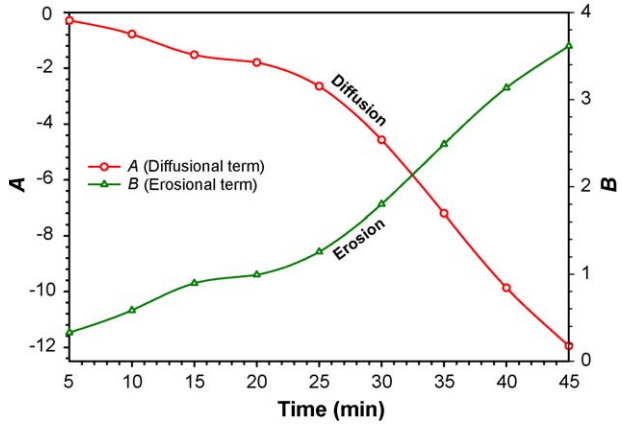

Fig. 4. Kopcha model parameters (A and B) versus time profile for optimized batch (experiment 20).

3.6. Characterization of optimal formulation

3.6.1. Fourier transform infra-red spectroscopy (FTIR)

FTIR spectra of κ-carrageenan powder, carrageenan blank beads, α-amylase loaded carrageenan beads, physical mixture of α-amylase and blank beads, and α-amylase are shown in Fig. 5. FTIR spectrum of κ-carrageenan powder showed various distinct peaks: very broad band spreading 3150–3600 cm^{-1} (strong; s) due to polyhydroxy $(-OH)_n$ group; 2968 cm^{-1} (s), 2920 cm^{-1} (s), and 2850 cm^{-1} (medium; m) due to C–H stretch; 1425 cm^{-1} (s) and 1375 cm^{-1} (s) due to C–H deformation; 1225 cm^{-1} (s) due to S=O stretch of sulfate ester salt; 1070 cm^{-1} due to C–O stretch of cyclic ethers; 925 cm^{-1} (s) due to C–O stretch of polyhydroxy groups attached to carbons; etc. Crosslinking of carrageenan by K^+ was shown by a decrease in the intensity of S=O stretch (1225 cm^{-1}) of sulfate ester group which was same as C–O stretch (1070 cm^{-1}) of cyclic ethers in intensity for the κ-carrageenan powder. This was probably because of some negatively charged sulfate ester reacted with positively charged K^+ and resulted in physicochemical changes of carrageenan. α-Amylase also showed various distinct peaks: one predominant band at 3190–3380 cm^{-1} (s) due to N–H stretch of secondary N-substituted amides; 2980 cm^{-1} (weak; w) due to C–H stretch, medium bands at 1500–1650 cm^{-1} due to C–C, while 898 cm^{-1} (s) and 875 cm^{-1} (s) due to p-substituted aromatic out of plane C–H deformation of aromatic residue of tryptophan or tyrosine; 2931 cm^{-1} (s) and 2898 cm^{-1} (s) due to

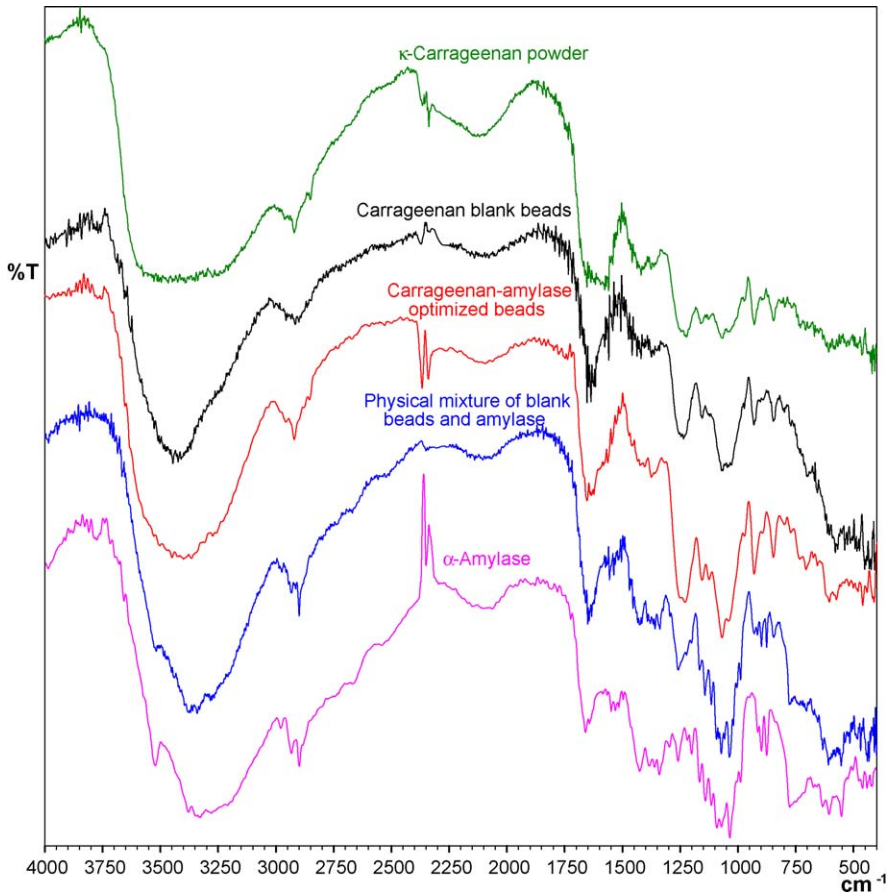

Fig. 5. The FTIR spectra of κ-carrageenan powder, carrageenan blank beads, α-amylase loaded carrageenan beads, physical mixture of α-amylase and blank beads, and α-amylase.

C–H stretch, while 1425 cm^{-1} (s), 1382 cm^{-1} (m), 1361 cm^{-1} (m), and 1340 cm^{-1} (m) due to C–H deformation of alkyl chain of amino acids; 1670 cm^{-1} due to C=O stretch of carboxylate anion and amide group; strong peaks between 1050 and 1200 cm^{-1}, weak bands at 550–600 cm^{-1}, and 400–450 cm^{-1} due to C–S stretch of sulfides and disulfides. With incorporation of α-amylase, the spectrum of beads was similar to that of the κ-carrageenan blank beads. However, the physical mixture of α-amylase and blank beads showed the peaks due to both α-amylase and κ-carrageenan. This confirms the amylase entrapment into the κ-carrageenan beads at molecular level.

3.6.2. *Differential scanning calorimetry (DSC)*

The DSC thermograms of potassium chloride, α-amylase, κ-carrageenan, blank beads, and α-amylase-loaded beads are shown in Fig. 6. Potassium chloride showed two non-significant exothermic peaks at 323 and 374 °C. α-Amylase exhibited three endothermic peaks at 148.5, 215.5, and 226.8 °C and one minor exothermic peak at 358 °C. Broad endothermic peak at 85 °C in the thermogram of κ-carrageenan was observed due to the presence of water molecules. Two minor peaks at 259 and 266 °C in the degradation exotherm of κ-carrageenan were absent in blank beads and α-amylase loaded beads, while major exothermic peak at 344 °C was found to be shifted towards higher temperature (355 °C) in blank beads. This showed that, κ-carrageenan-KCl beads are more stable than κ-carrageenan. However, additional two peaks (one endothermic at 207 and one exothermic at 226.5 °C) were observed in the thermogram of blank beads due to the potassium-κ-carrageenan interaction. DSC thermogram of enzyme loaded beads was similar to that of blank beads except all corresponding peaks were shifted to lower temperature, might be due to the presence of α-amylase. However, it did not showed any peak analogous to α-amylase. This confirms that most of the enzyme was uniformly dispersed at the molecular level in the beads.

3.6.3. *Morphology of the beads*

The spherical shape of beads in wet state was usually lost after drying especially for beads prepared with low carrageenan concentration. In 2.5% (w/v) carrageenan, the dried beads were very irregular and tend to agglomerate due to low mechanical strength. With the increase of κ-carrageenan concentration (3.5%, w/v), the shape of beads retained considerably. However, the shape of beads changed to disc with a collapsed center (Fig. 7) during drying process due to aggregation of the helical fibers into bundles and the squeezing out of some water from the gel (Iborra et al., 1997). Normally the spherical shape was retained when the carrageenan concentration was as high as 5.0% (w/v), but viscosity of 5.0% (w/v) solution was too high for bead preparation under present

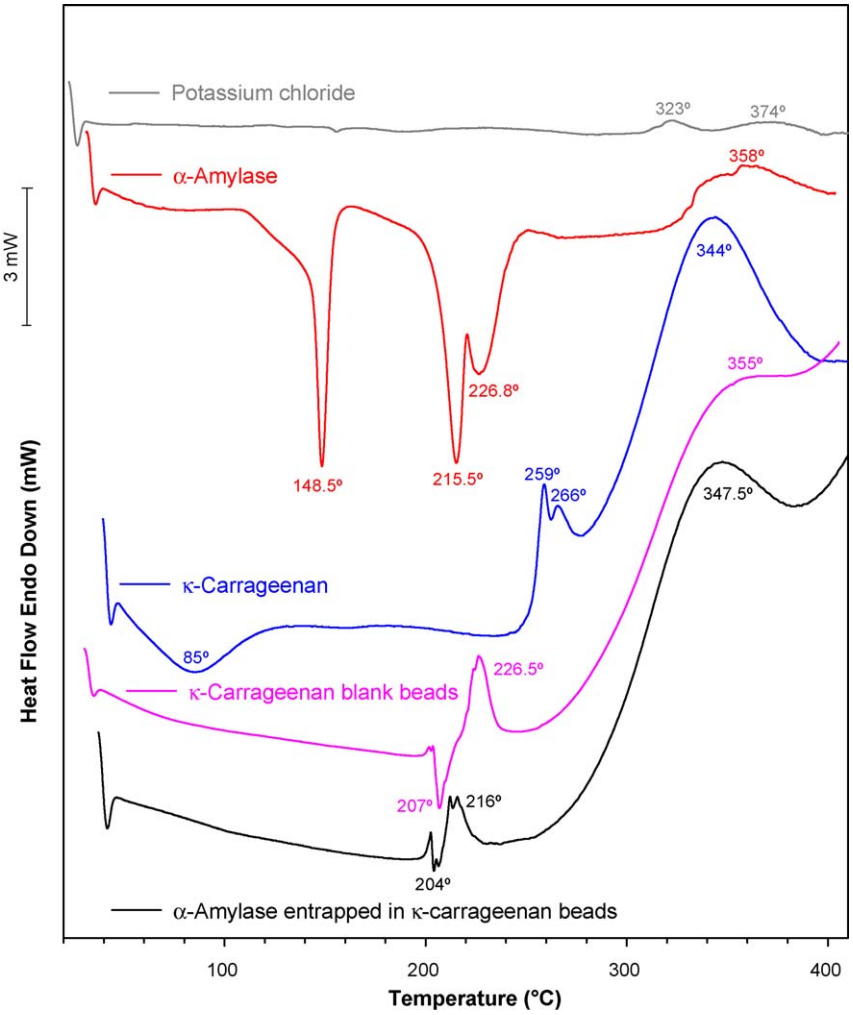

Fig. 6. The DSC thermograms of potassium chloride, α-amylase, κ-carrageenan powder, blank beads, and α-amylase loaded carrageenan beads made at the same analytical conditions.

experimental conditions so it was not studied. Crosslinked hydrogels reach an equilibrium swelling level in aqueous solutions, which depends mainly on the crosslink density. In some cases, depending on the solvent composition, temperature and solids concentration during gel formation, phase separation can occur, and water-filled 'voids' or 'macropores' can form which can be observed Fig. 2. One noticeable characteristic of the beads' surface is high degree of crosslinking when the concentration of potassium chloride increased (Fig. 2A–C). Further, the surface morphology was improved (i.e. decrease in roughness) with increase in κ-carrageenan concentration (Fig. 2D–F) due to the high viscosity of the κ-carrageenan solution.

3.7. Stability study

For the formulation developed, the similarity factor (f_2) was calculated by a comparison of the dissolution profiles at each storage condition with the control at the initial condition. Results of f_2 factors ranged from 73 to 97 with 2–5% average difference. Overall, results from the stability studies indicated that capsules were physically and chemically stable for at least 12 months at $40 \pm 2\,^{\circ}C/75 \pm 5\%$ relative humidity and for more than 12 months (approximately for double time period) at $30 \pm 2\,^{\circ}C/65 \pm 5\%$ relative humidity.

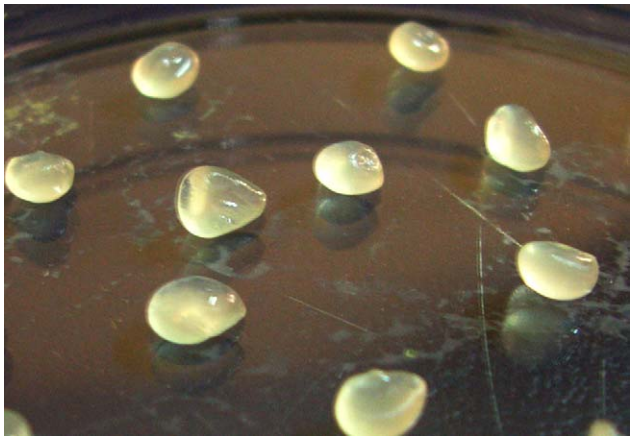

Fig. 7. Photograph of wet κ-carrageenan beads showing spherical disk shape with collapsed center during drying process.

Table 6
Comparison of different dissolution kinetics models

ES[a]	Release model										
	Zero-order		First-order		Higuchi matrix		Korsmeyer–Peppas			Hixson–Crowell	
	K_0	r_0	K_1	r_1	K_H	r_H	n	K_k	r_k	K_s	r_s
9	3.19	0.97	−0.11	0.74	14.13	0.87	1.30	1.22	0.98	−0.02	0.87
13	2.53	0.96	−0.08	0.90	13.06	0.87	1.33	0.83	0.97	−0.02	0.94
2	2.31	0.96	−0.07	0.85	11.91	0.84	1.62	0.27	0.98	−0.01	0.92
24	2.33	0.96	[b]	[b]	12.04	0.85	1.38	0.61	0.97	−0.02	0.87
17	2.08	0.96	[b]	[b]	10.87	0.82	1.56	0.27	0.98	−0.02	0.82
6	1.75	0.95	[b]	[b]	10.30	0.83	1.71	0.12	0.97	−0.01	0.90
1	1.79	0.96	−0.06	0.86	10.60	0.84	1.50	0.27	0.97	−0.01	0.92
27	1.65	0.94	−0.05	0.83	9.68	0.81	1.94	0.04	0.98	−0.01	0.90
10	1.51	0.93	−0.05	0.79	8.93	0.78	2.21	0.01	0.96	−0.01	0.87
23	2.18	0.97	[b]	[b]	11.38	0.85	1.29	0.76	0.98	−0.02	0.84
8	1.93	0.95	−0.06	0.76	10.18	0.81	1.50	0.29	0.98	−0.01	0.86
15	1.65	0.95	−0.05	0.83	9.74	0.81	1.81	0.07	0.99	−0.01	0.90
12	1.86	0.94	−0.06	0.72	9.83	0.79	1.47	0.30	0.97	−0.01	0.83
26	1.66	0.94	−0.05	0.85	9.78	0.81	2.00	0.04	0.99	−0.01	0.90
19	1.32	0.92	−0.04	0.90	9.15	0.83	2.03	0.02	0.97	−0.01	0.92
3	1.50	0.94	[b]	[b]	8.90	0.79	1.81	0.06	0.97	−0.01	0.80
18	1.24	0.93	−0.05	0.86	8.59	0.81	2.04	0.02	0.97	−0.01	0.91
21	1.16	0.94	−0.04	0.84	8.09	0.80	2.14	0.01	0.94	−0.01	0.91
4	1.70	0.96	[b]	[b]	10.10	0.84	1.40	0.35	0.97	−0.01	0.89
25	1.55	0.95	−0.05	0.80	9.24	0.81	1.64	0.12	0.97	−0.01	0.88
11	1.25	0.94	[b]	[b]	8.73	0.82	1.77	0.05	0.96	−0.01	0.91
22	1.47	0.94	−0.05	0.71	8.83	0.80	1.69	0.09	0.98	−0.01	0.85
14	1.24	0.94	−0.04	0.88	8.61	0.82	2.01	0.02	0.98	−0.01	0.92
7	1.16	0.93	−0.04	0.86	8.02	0.80	2.42	0.00	0.98	−0.01	0.91
5	1.17	0.94	−0.04	0.82	8.17	0.81	1.61	0.08	0.96	−0.01	0.91
16	1.09	0.93	−0.04	0.79	7.58	0.79	2.22	0.01	0.97	−0.01	0.89
20	1.02	0.93	−0.03	0.80	7.13	0.78	2.23	0.00	0.95	−0.01	0.88

[a] ES, experimental sequence.
[b] Not possible.

An approach for analyzing the data on a quantitative attribute that is expected to change with time is to determine the time at which the 95% one-sided confidence limit for the mean curve intersects the acceptance criterion (not more than 5% change in assay from its initial value). The accelerated stability data for prepared formulation, marketed formulation and the bulk α-amylase were extrapolated to calculate the shelf-life (Fig. 8) and were found be 3.53, 0.99 and 0.41 year, respectively. Hence, the stability of the entrapped α-amylase was significantly improved than that of the conventional dosage forms.

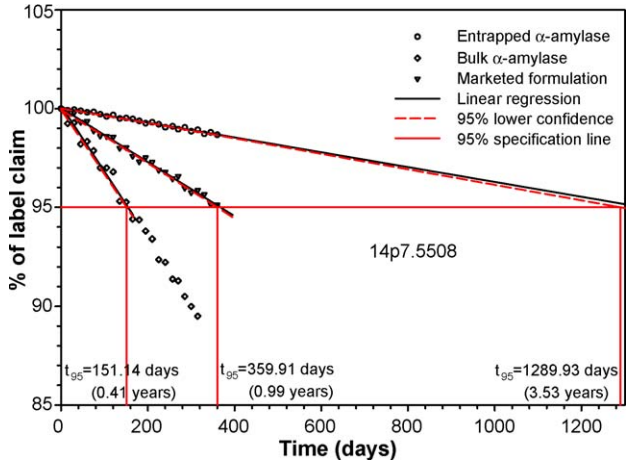

Fig. 8. Extrapolation of accelerated stability data for shelf-life calculation.

4. Conclusions

Ionotropically corsslinked κ-carrageenan beads exhibit promising stability improvement of entrapped α-amylase and can find a place in the design of multiparticulate drug delivery systems. The optimization of the process using the composite index resulted in more than 73% entrapment and more than 74 min of T_{90} at high levels of all three process variables. T_{50} and T_{90} were increased with increase in all three process variables. Percentage entrapment and particle size were found to be directly proportional to κ-carrageenan concentration and inversely proportional to potassium chloride concentration and hardening time. Mathematical analysis of the different drug release modalities has evidenced that enzyme release from carrageenan beads follows Korsmeyer–Peppas' power law equation with super case-II transport mechanism. Furthermore, investigation of release profile by Kopcha model revealed that enzyme release is due to erosion and not by diffusion. FTIR and DSC study showed uniform dispersion of α-amylase at molecular level in the carrageenan beads. Texture analysis discovered directly proportional relation of degree of crosslinking with

potassium chloride concentration. In addition, the surface roughness decreased with increase in κ-carrageenan concentration. Accelerated and long term stability study illustrated considerably improved shelf-life of α-amylase entrapped in carrageenan than the conventional dosage form. The application of a single polymer (as used traditionally) for the formation of beads allows the formulator to predict and produce beads of different geometries, strengths and release characteristics. Results of presented experiments seem to be of value for the pharmaceutical industries associated with digestive enzymes formulations.

Acknowledgements

This research was supported by a grant from the All India Council for Technical Education (New Delhi, India, 8019/RDII/R&D/PHA (207)/2000–2001), for which Dr. R.C. Mashru was the principal investigator. We acknowledge the University Grants Commission (New Delhi, India) for availing Senior Research Fellowship to Mr. Mayur G. Sankalia. We greatly appreciate the Vaibhav Analytical Services Ltd. (Ahmedabad, India) for skillful assistance and providing FTIR testing facility in this study.

References

Bhardwaj, S.B., Shukia, A.J., Collins, C.C., 1995. Effect of varying drug loading on particle size distribution and drug release kinetics of verapamil hydrochloride microspheres prepared with cellulose esters. J. Microencapsul. 12, 71–81.

Bickerstaff, G.F., 1997. Immobilization of enzymes and cells: some practical considerations. In: Bickerstaff, G.F. (Ed.), Immobilization of Enzymes and Cells, Methods in Biotechnology, vol. 1. Humana Press, Totowa, New Jersey, pp. 1–12.

Bodeam, X., Leucata, S.E., 1997. Optimization of hydrophilic matrix tablets using a D-optimal design. Int. J. Pharm. 153, 247–255.

Bodmeier, R., Wang, J., 1993. Microencapsulation of drugs with aqueous colloidal polymer dispersions. J. Pharm. Sci. 82, 191–194.

Bonferoni, M.C., Rossi, S., Tamayo, M., Pedraz, J.L., Dominguez Gil, A., Caramella, C., 1994. On the employment of λ-carrageenan in a matrix system. II. λ-Carrageenan and hydroxypropylmethylcellulose mixtures. J. Control. Rel. 30, 175–182.

Chen, H., Langer, R., 1997. Magnetically-responsive polymerized liposomes as potential oral delivery vehicles. Pharm. Res. 14, 537–540.

Derringer, G., Suich, R., 1980. Simultaneous optimization of several responses variables. J. Qual. Technol. 2, 214–219.

Garcia, A.M., Ghaly, E.S., 1996. Preliminary spherical agglomerates of water soluble drug using natural polymer and cross-linking technique. J. Control. Rel. 40, 179–186.

Gibaldi, M., Feldman, S., 1967. Establishment of sink conditions in dissolution rate determinations - theoretical considerations and application to non-disintegrating dosage forms. J. Pharm. Sci. 56, 1238–1242.

Gohel, M.C., Patel, M.M., Amin, A.F., 2003. Development of modified release diltiazem HCl tablets using composite index to identify optimal formulation. Drug Dev. Ind. Pharm. 29, 565–574.

Guzman-Maldano, H., Paredes-Lopez, O., 1995. Amylolytic enzymes and products derived from starch; a review. Crit. Rev. Food. Nutr. 36, 373–403.

Higuchi, T., 1963. Mechanism of sustained-action medication. Theoretical analysis of rate of release of solid drugs dispersed in solid matrices. J. Pharm. Sci. 52, 1145–1149.

Hixson, A.W., Crowell, J.H., 1931. Dependence of reaction velocity upon surface and agitation. Ind. Eng. Chem. 23, 923–931.

Hossain, K.S., Miyanaga, K., Maeda, H., Nemoto, N., 2001. Sol–gel transition behavior of pure ι-carrageenan in both salt-free and added salt states. Biomacromolecules 2, 442–449.

Hsiu, J., Fischer, E.H., Stein, E.A., 1964. Alpha-amylase as calcium-metalloenzymes. II. Calcium and the catalytic activity. Biochemistry 3, 61–66.

Iborra, J.L., Manjon, A., Canovas, M., 1997. Immobilization in carrageenans. In: Bickerstaff, G.F. (Ed.), Immobilization of Enzymes and Cells, Methods in Biotechnology, vol. 1. Humana Press, Totowa, New Jersey, pp. 53–60.

Kopcha, M., Lordi, N., Tojo, K.J., 1991. Evaluation of release from selected thermosoftening vehicles. J. Pharm. Pharmacol. 43, 382–387.

Korsmeyer, R.W., Gurny, R., Doelker, E.M., Buri, P., Peppas, N.A., 1983. Mechanism of solute release from porous hydrophilic polymers. Int. J. Pharm. 15, 25–35.

Nielsen, J.E., Beier, L., Otzen, D., Borchert, T.V., Frantzen, H.B., Andersen, K.V., Svendsen, A., 1999. Electrostatics in the active site of an α-amylase. Eur. J. Biochem. 264, 816–824.

Pather, S.I., Russell, I., Syce, J.A., Neau, S.H., 1998. Sustained release theophylline tablets by direct compression. Part 1. Formulation and in vitro testing. Int. J. Pharm. 164, 1–10.

Peppas, N.A., 1985. Analysis of Fickian and non-Fickian drug release from polymers. Pharm. Acta Helv. 60, 110–111.

Picker, K.M., 1999. Matrix tablets of carrageenans. II. Release behavior and effect of added cations. Drug Dev. Ind. Pharm. 25, 339–346.

Prestwich, G.D., Marecak, D.M., Marecak, J.F., Vercruysse, K.P., Ziebell, M.R., 1998. Controlled chemical modification of hyaluronic acid. J. Control. Rel. 53, 93–103.

Rice, E.W., 1959. Improved spectrophotometric determination of amylase with a new stable starch substrate solution. Clin. Chem. 5, 592–596.

Ritger, P.L., Peppas, N.A., 1987. A simple equation for description of solute release. II. Fickian and anomalous release from swellable devices. J. Control. Rel. 5, 37–42.

Schmidt, A.G., Wartewig, S., Picker, K.M., 2003. Potential of carrageenans to protect drugs from polymorphic transformation. Eur. J. Pharm. Biopharm. 56, 101–110.

Shigeo, O., Toshihiko, K., Yousuke, M., Horoshima, S., Kozo, T., Nagai, T., 1994. A new attempt to solve the scale up problem for granulation using response surface methodology. J. Pharm. Sci. 83, 439–443.

Sipahigil, O., Dortunc, B., 2001. Preparation and in vitro evaluation of verapamil HCl and ibuprofen containing carrageenan beads. Int. J. Pharm. 228, 119–128.

Smith, B.W., Roe, J.H., 1957. A micromodification of the Smith and Roe method for the determination of amylase in body fluids. J. Biol. Chem. 227, 357–362.

Suzuki, S., Lim, J.K., 1994. Microencapsulation with carrageenan-locust bean gum in a multiphase emulsification technique for sustained drug release. J. Microencapsul. 11, 197–203.

Taylor, M.K., Ginsburg, J., Hickey, A.J., Gheyas, F., 2000. Composite method to quantify powder flow as a screening method in early tablet or capsule formulation development. AAPS PharmSciTech 1, article 18 (http://www.pharmascitech.com).

Uhlig, H., 1998. Description of Enzymes. in: Industrial Enzymes and their Applications. A Wiley-Intersciences Publication John Wiley & Sons. Inc., New York, pp. 37–202.

Uitdehaag, J.C., Mosi, R., Kalk, K.H., van der Veen, B.A., Dijkhuizen, L., Withers, S.G., Dijkstra, B.W., 1999. X-ray structures along the reaction pathway of cyclodextrin glycosyltransferase elucidate catalysis in the α-amylase family. Nat. Struct. Biol. 6, 432–436.

Wagner, J.G., 1969. Interpretation of percent dissolved-time plots derived from in vitro testing of conventional tablets and capsules. J. Pharm. Sci. 58, 1253–1257.